JOURNAL OF MATERIALS SCIENCE **34** (1999) 881–886

Structure of zinc–nickel alloyelectrodeposits

BRUET-HOTELLAZ, J. P. BONINO, A. ROUSSET
Laboratoire de Chimie des Matériaux Inorganiques, URA CNRS 1311, Université Paul-Sabatier, 31062 Toulouse Cedex, France
E-mail: bonino@iris.ups-tlse.fr

MAROLLEAU, E. CHAUVEAU
LEDEPP—SOLLAC, 57191 Florange, France

Zinc–nickel alloys with 0 to 13 wt % of nickel were electrodeposited from a chloride bath. The structure and microstructure change of as-deposited alloys versus the nickel content in the deposits is shown here. From X-ray diffraction an electrodeposited phase diagram in which the substitution of Zn by Ni atoms in η or γ structure induces a lattice distortion has been defined. In contrast to the thermodynamic phase diagram, the δ phase does not appear in as-deposited coatings. Two composition ranges have been defined, the first of which corresponds to the formation of a solid solution sursaturated in nickel (η_d) for the alloys containing up to 7.4 wt % of nickel. The second, corresponds to the formation of a γ phase out of equilibrium unsaturated in nickel. For an increase in nickel, the added atoms are preferentially incorporated into this unsaturated γ phase, and the η_d phase gradually disappears up to 13 wt % of nickel. The δ phase is obtained in electrodeposited alloys only after heat treatment at 200 °C. The δ phase recrystallized from metastable phases η_d and γ_d.

1. Introduction

ZnNi alloy electrodeposits are of considerable interest as corrosion resistant coatings for automobile steel bodies. Several different corrosion tests, commonly used to evaluate the corrosion resistance of electrodeposited coatings, indicate that alloying nickel (8–14 wt %) with zinc, improves the corrosion protection by a factor of 6 or 7 compared to pure zinc [1–4]. However, the optimum nickel content in the deposits and the corresponding structure required to provide maximum corrosion resistance by sacrificial behaviour is not well established, in particular the critical phase identification and phase distribution mapping. The crystal structure of the deposits is a matter of debate in the range of 0–15 wt % of nickel. Many authors [5–8] have reported that the phases contained in as deposited ZnNi alloys are in good agreement with those obtained at thermodynamic equilibrium. However, some authors [2, 4, 9, 10, 11] have proposed an electrodeposited ZnNi alloy phase diagram in which ZnNi phases are metastable and generally exhibit fewer phases existing over a wider range of nickel composition. For example, Lambert *et al.* [2] compare the structure of as-deposited ZnNi coatings containing up to 38 weight percent of nickel with those predicted by the equilibrium phase diagram. More recently, many studies reported by Japanese scientists [9–11] have focused on the structure of ZnNi alloy obtained from the sulphate bath in the range 0–10 wt % of nickel. The η phase with hcp structure is formed up to 6% of nickel content, while the γ phase with a brass structure is obtained in the range of 6 to 10 wt % of nickel. In brief, their principal disagreement is about the presence of the δ phase around 10 to 12 wt % of nickel in electrodeposited alloys.

In this paper, the structure and microstructure change of as-deposited ZnNi alloys obtained from the chloride bath between 0 to 13 wt % of nickel is presented. Furthermore, it is shown that the metastable phases obtained in as-deposited alloys can be transformed in the δ phase after heat treatments up to 250 °C.

2. Experimental conditions

The experimental apparatus used for the electrodeposition was made up of a cylindric cell containing 250 cm^3 of electrolyte solution. A rotating disk electrode (RDE) was used to agitate the electrolyte solution at 1250 rpm. The cathode was a low carbon steel disk of 0.8 cm^2 surface area, and the anode was a platinum disk with 1 cm^2 surface area. Before immersion, the steel surface was cleaned with hydrochloric acid (140 g/1) and rinsed with deionised water. The ZnNi alloy deposits were obtained at 60 °C from chloride based electrolyte containing $ZnCl_2$, $NiCl_2$, $6H_2O$, KCl, and an organic additive. In order to obtain ZnNi alloy deposits with varying nickel content, the nickel concentration of the electrolyte was varied from 0 to 13,5 wt %. The electrolyte solution was prepared using deionised water and analytical grade chemicals. The electrolyte pH was adjusted to $4{,}5 \pm 0.02$. Electrodepositions were carried out under galvanostatic conditions at high current density (110 A/dm^2). After plating, the disk cathode

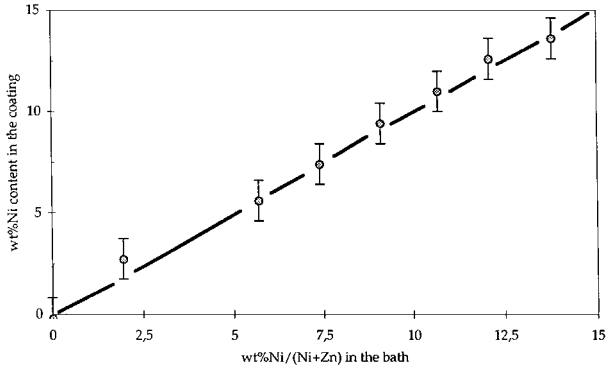

Figure 1 Variation of Ni content in the coatings versus the Ni/Ni+Zn ratio in the bath.

was immediately washed with deionised water and air dried. The thickness of each coating measured around 10 μm. The structure of as-deposited coatings was determined by X-ray diffraction with grazing incidence of 1° and with Cu anticathode ($\lambda = 1.5415$ Å). After heat treatments at 100 °C, 200 °C, and 250 °C, phase identification was also performed from X-ray diffraction patterns. Electron microprobe analysis technique with a Cameca SX 50 was used to determine coating composition in the as-deposited state. First, each coating was polished using successively diamond solutions with 9 μm, 3 μm, and 1 μm powders. Ten measurements were carried out on each sample. The morphology of the deposit was observed by scanning electron microscopy (SEM) with a JEOL apparatus.

3. Results

The influence of Ni^{++} concentration on electroplate composition is shown in Fig. 1. From the Brenner classification, it can be said that, for the electrolytic conditions used, the simultaneous deposition of nickel and zinc results from an equilibrium type codeposition process because the ratio of Ni in the deposits is always the same as that in the electrolyte solution.

3.1. Microstructure

The microstructure of the zinc deposits, observed by SEM, changed clearly with the increase in the quantity of nickel codeposited with zinc (Fig. 2). Agglomerates of platelets arranged without apparent order constituted the pure zinc coatings. A decrease in grain size appeared by alloying effect when a low quantity of nickel was introduced into the deposits (2.8 wt % of Ni). The microstructure was composed of small grains with a more isotropic shape.

When the nickel content reached 7.4 wt %, we observed that the grains presented a marked hexagonal shape characteristic of the growing mode in the c-axis direction (Fig. 2c). This orientation could result from the growth of the pyramidal (101) plane or basal (001) plane. As shown in Fig. 2d, each grain is composed of a hexagonal cylinder with the characteristic shape of a pyramidal crystal to the growth mode from the pyramidal (101) plane, Y. Ohmori *et al.* [10] described the growth of the hexagonal grains as a homoepitaxial growth in a side-by-side fashion in the c axis direction, leading to the formation of grains with a hexagonal cylinder shape enclosed (001) and (100) planes.

The increase in nickel content up to 13 wt % involved a new decrease in grain size with simultaneous appearance of roughness, but the hexagonal section of the grains was partly conserved (Fig. 2e). Beyond 13 wt % of Ni, the deposits covered more, the roughnesses disappeared, and the shape of the grains was not so well defined (Fig. 2f).

This microstructural characterization has shown three ranges of microstructure defined from two characteristic nickel contents. The first one, up to 7.4 wt % of nickel, corresponds to the formation of grains with a hexagonal shape, with characteristic growth mode in the c axis direction. The second one, up to 13 wt % of nickel, corresponds to the disappearance of the hexagonal shape of the grains. The final one, above 12.5 wt %, corresponds to a deposit with finer grains and with improved coverage.

3.2. Structure

The structural variation of ZnNi alloys versus nickel content in coatings is illustrated in Fig. 3 by the X-ray patterns. Some peaks of Fe substrate appear in addition to the Zn-Ni one. Two structures of the Zn-Ni alloy can be distinguished; hcp η phase crystallized up to 12 wt % of Ni with a distorted lattice, while cubic body-centered γ phase, clearly identified from the JCPDS card n°6-653, appeared from 7,4 wt % of Ni. The data on the X-ray patterns of the δ phase given in the literature do not allow its identification.

The X-ray pattern of the pure Zn coating was very clear and agreed exactly with the hcp structure of Zn JCPDS card n°4-831. The η hcp structure of pure Zn is naturally distorted as compared to the hcp structure of Co, Mg, Ti, or Be. This distortion, also obtained in electrodeposited zinc, results from the ellipsoïdal shape of the electronic cloud of Zn. As a result, the c parameter is higher and the a parameter smaller than in the theoretical hcp structure. Consequently, the c/a ratio, equal to 1.856, is higher than the theoretical value (1,633) of Co, Mg, Ti, or Be.

From the low quantities of zinc substituted by nickel, the structural modifications of the zinc alloys complicate the identification of the diffraction peaks related to the η phase. The X-ray patterns of the coating containing a low nickel content, close to 2.8 wt %, showed a broadening of the diffraction peaks. This broadening can be explained by a refining microstructure as seen in the microstructure study. In Fig. 3a significant shift of the peaks of the η hcp structure is depicted. In Table I, the variation of lattice spacing when the nickel content in the deposit increases up to 10 wt % is shown. The values related to the interreticular planes parallel or close to the basal plane of the η phase, respectively (002), (102), and (103), decreased when the nickel content in the deposits increased. In contrast, the lattice spacing of the parallel planes or close to the orientation of prismatic planes increased, respectively (10 0), (110), and (201). These variations of interreticular spacing can be explained by the substitution of zinc atoms by

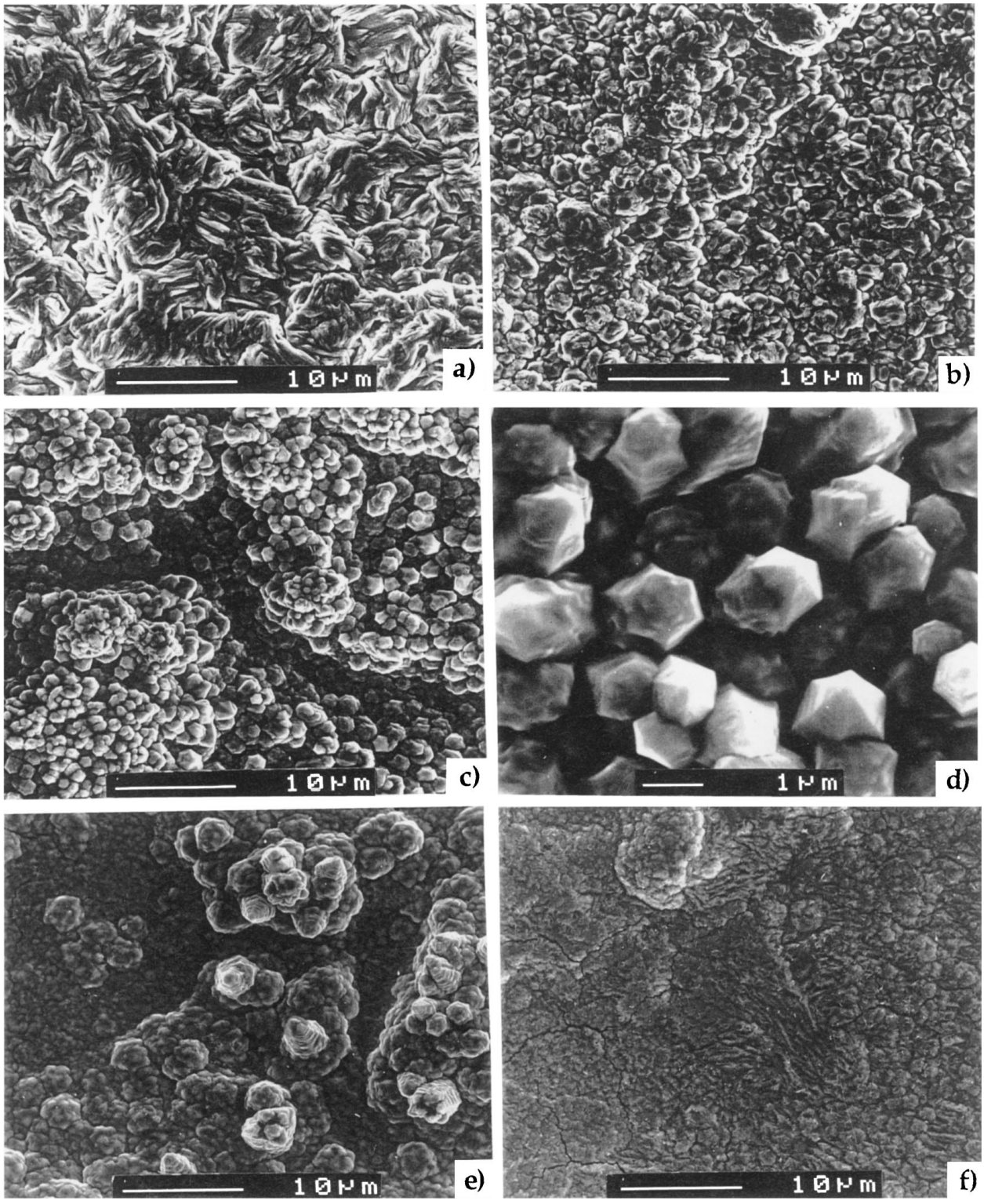

Figure 2 Variation of the microstructure of the coatings versus Ni content; (a) 0, (b) 2.8, (c) and (d) 7.4, (e) 10, and (f) 13.5 wt % of Ni.

nickel atoms. In fact, the electronic cloud of the Ni atom is not distorted, and its atomic radius is less than the atomic radius of Zn ($r_{Ni} = 1.25$ Å, $r_{Zn} = 1.37$ Å). In these conditions, we can easily understand that the substitution of Zn by Ni atoms consequently modifies the lattice parameters of the η structure of Zn (Fig. 4). The *c* parameter, therefore, decreases rapidly and the *a* parameter increase slowly as the Ni content increases. Thus, the hcp structure of the η phase returns to the more stable hcp structure at 7.4 wt % of Ni, which has a c/a ratio close to the theoretical hcp 1.633 (Fig. 5). This linear variation of the *a* and *c* parameters up to 7.4 wt % of Ni content can be explained by the formation of an ideal solid solution from the η hcp phase. The same evolution of η phase lattices parameters up to 6 wt % of Ni in coatings has been reported by Seki *et al.* [9]. A similar deformation has been observed by Massalski *et al.* [12], who studied the changes of lattice spacing and axial ratio of hcp phases contained in zinc alloys with noble metals such as Cu, Ag and Au.

The value 7.4 wt % of nickel in the deposit is thus critical and corresponds to the maximum of nickel

TABLE I Variation of interreticular distances (Å) of η and γ structures versus Ni content in the coatings

%Ni mas	0	2,8	7,4	10	12,5
η(002)	2,4705	2,361	2,1765	2,1683	
η(100)	2,305	2,3398	2,3832	2,4134	
γ(411–330)			*2,1126*	*2,1144*	*2,1018*
η(101)	2,0889	2,0904	2,096		
γ(422)				1,8248	
η(102)	1,685	1,6583	1,6083	1,6068	
γ(442–600)			*1,487*	*1,4892*	*1,4846*
η(103)	1,3395	1,3056	1,2396	1,2437	
η(110)	1,3302	1,3469	1,3768		
γ(444)				*1,2772*	*1,2846*
η(004)	1,2343				
γ(552–633)			*1,2192*	*1,2216*	*1,2143*
η(200)	1,1517				
η(201)	1,1216	1,1337			
η(104)	1,0881				
γ(554–811)			*1,0941*	*1,0954*	*1,0982*
γ(822)				*1,0577*	*1,0511*
η(202)	1,0441	1,0467	1,0486	1,0486	

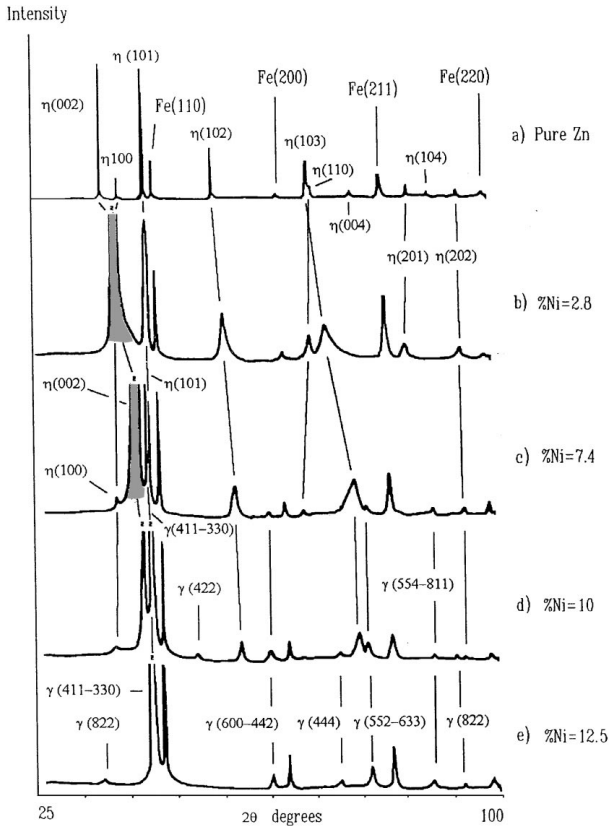

Figure 3 Structural change of the coatings versus Ni content. X-ray patterns were obtained with grazing incidence at 1° and Cu anticathode (λ_{Cu} =1.5415 Å).

substituted in the zinc η_d phase. In this value, for which the c/a ratio of η_d phase is close to the theoretical value of the c/a ratio of the hexagonal close packed structure, the presence of grains with very marked hexagonal shape also was observed by SEM.

Beyond 7.4 wt % of Ni content, the c/a ratio of the η_d phase was constant at around 1.58, and some peaks characteristic of the γ phase appeared. From this value, the deposits were two-phased. The η_d phase of zinc had attained the maximum of saturation in nickel, and all

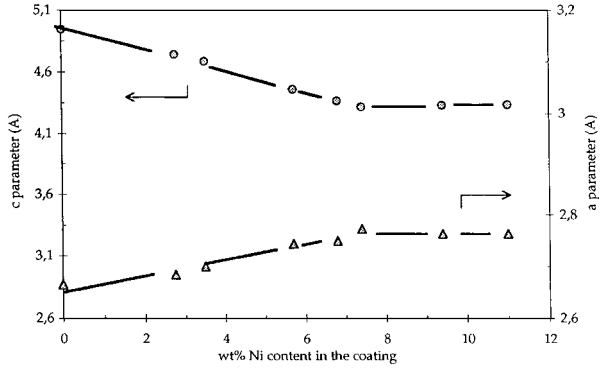

Figure 4 Variation of the *a* and *c* parameters of the γ structure according to the Ni content in the coating.

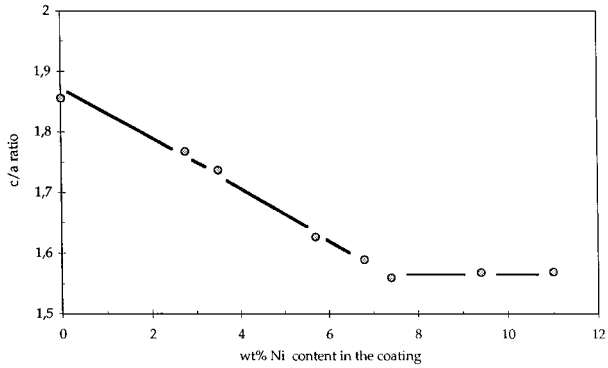

Figure 5 Variation of the c/a ratio of the η structure according to the Ni content in the coating.

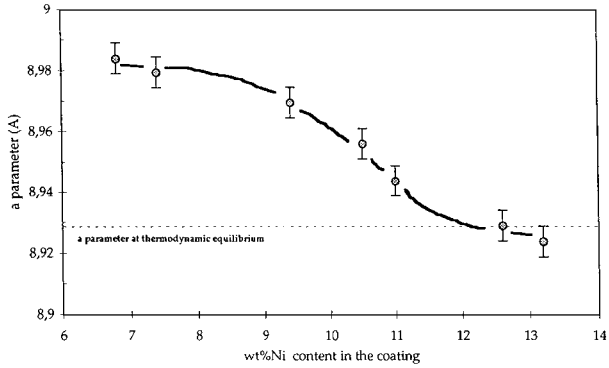

Figure 6 Variation of lattice parameters of the γ structure according to the Ni content in the coating [with (600) and (552) planes].

the nickel introduced beyond 7.4 wt % contributed to the electrocrystallization of the γ phase. The latter increased while the η_d phase gradually disappeared up to 12.5 wt % of nickel in the deposit. Thermodynamically, the Zn-Ni γ phase only appeared beyond 12.5 wt % of nickel. Electrodeposited alloys containing between 7.4 and 12.5 wt % of Ni are therefore out of thermodynamic equilibrium and are constituted with two phases, among which the γ_d phase is probably depleted in nickel. The evolution of lattice parameter a of the γ_d structure versus to Ni content in alloys confirms the above. It is evaluated by two individual peaks of the γ_d phase (i.e., (600) and (552) planes) from X-ray patterns. The γ_d phase of the alloys containing 7.4 wt % of Ni has a lattice parameter higher than the one obtained at thermodynamic equilibrium. As previously stated, the

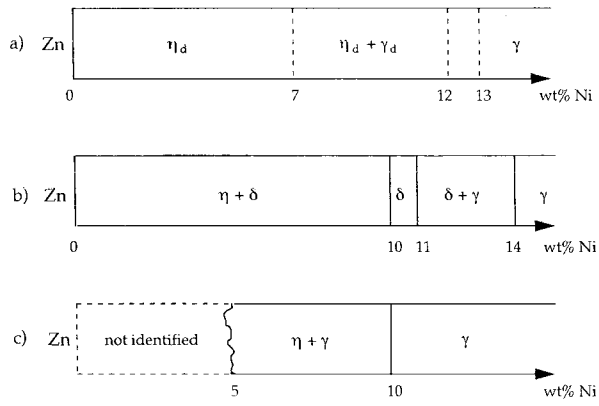

Figure 7 Zn-Ni phase diagrams, (a) electrodeposited (present work), (b) at thermodynamic equilibrium, and (c) proposed by Lambert (c) [2].

radius of the Zn atoms is higher than that of Ni, the supersaturation in Zn of the γ_d phase contained in $Zn_{92.6}Ni_{7.4}$ alloy can explain the high value of the lattice parameter. When the Ni content in the deposits increased from 7.4 to 12.5 wt %, the lattice parameter decreased up to the theoretical value. Beyond this value the alloys are monophased γ.

From these results, an electrodeposited phase diagram of Zn-Ni alloys can be defined. Fig. 7 compares this to, to the thermodynamic phase diagram. The main difference is the absence of the δ phase in the electrodeposited alloys (also reported by Lambert *et al.* [2]). In this case, the presence of η_d and γ_d phases out of thermodynamic equilibrium in a composition range of between 7.4 and 12.5 wt % of nickel is shown.

3.3. Annealing effect

In the aim to confirm the out-of-equilibrium state of electrodeposited alloys containing between 2.8 and 13.5 wt % of nickel, several heat treatments at various temperatures were performed.

The X-ray diffraction patterns of alloys after annealing at 100, 200, and 250 °C are illustrated in Fig. 8. The alloys selected for this study contained 2.8, 7.4, 10, and 13,5 wt % of nickel. The annealing treatment of the alloys containing supersaturated η_d phase and depleted γ_d, involved a precipitation of a new phase, different to η and γ, that could be the δ phase. However, the structure of the δ phase at thermodynamic equilibrium is not very clear. Several structures are suggested in the literature such as hexagonal [13], tetragonal (JCPDS card n°10-209), or monoclinic [14] structure. More recently, O. Bardin [15] has synthesized using metallurgical techniques, which are alloys with the stoichiometric composition of the pure δ and γ phases (Fig. 9). The diffraction patterns of the δ phase obtained by this author cannot be attributed to the structure suggested by the literature data. For the following investigations, this diffraction pattern to be that of the δ phase will be used for consideration. It can be seen in the diffraction patterns shown in Fig. 9a–d, that whatever the deformed phases η_d and γ_d present in the as-deposited coating, the first transformation appearing after annealing at 200 °C

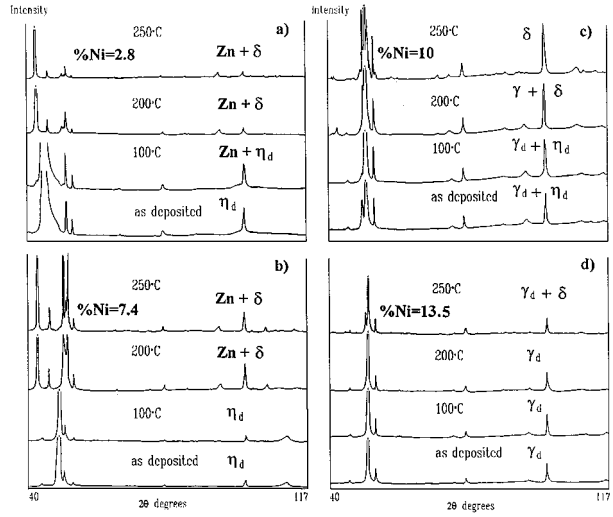

Figure 8 Structural change after annealing at different temperatures for coatings with (a) 2.8, (b) 7.4, (c) 10, and (d) 13,5 wt % of Ni. X-ray patterns were obtained with $\theta/2\theta$ technique and with Co anticathod ($\lambda_{Co} = 1{,}7902$ Å).

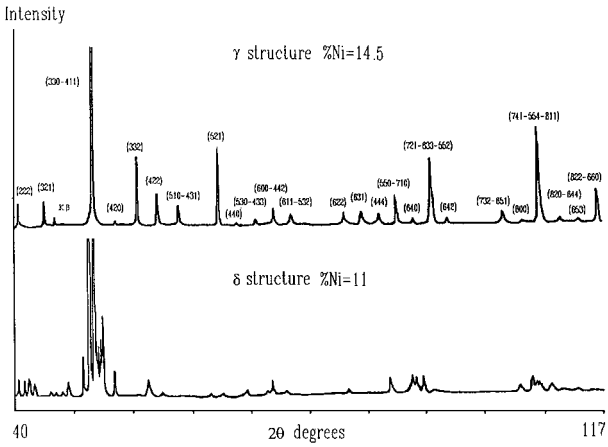

Figure 9 X-ray patterns of the γ and δ structures obtained with $\theta/2\theta$ technique and with Co anticathod ($\lambda_{Co} = 1{,}7902$ Å). The samples were prepared under equilibrium conditions [15].

was the precipitation of the δ phase. The precipitation of the δ phase was very clear for the alloy containing the quantity of nickel corresponding to the composition range of the thermodynamic diagram (10 to 11 wt %) (c). The η_d structure disappeared completely at 200 °C and at the same time, the γ_d structure grew richer in zinc atoms up to the critical Ni content of the δ phase. The transformation was complete at 250 °C. When the nickel content in deposit was outside these values, the peaks of the δ phase decreased in intensity to the advantage of the η phase; when the nickel content is lower (a and b) or γ phase when the nickel content was higher (d). For the lower Ni content (a and b), the zinc and δ structures precipitated from the η_d phase; and for the higher Ni content (d), the δ phase came from the γ_d phase.

4. Conclusion

Zn-Ni phases obtained from electrodeposition technology are not in thermodynamic equilibrium. The electrodeposited phase diagram, in the range of 0 to 13 wt % of nickel, is different from the thermodynamic diagram.

The difference is due to the absence of the δ phase in electrodeposited alloys. The electrodeposited phase diagram can be divided into two composition ranges. The first corresponds to the alloys containing up to 7.4 wt % of nickel, in which the substitution of Zn by Ni atoms in the η structure induces a lattice distortion. Beyond this value, a distorted γ_d phase appears for nickel contents lower than that predicted by the thermodynamic equilibrium phase diagram. The presence of these two phases out of thermodynamic equilibrium is at the origin of the δ phase precipitation observed after annealing at 200 °C.

References

1. H. L. HARVIE in "Zn-Based Steel Coating Systems: Metallurgy & Performance," edited by J. Krauss and D. K. Matlock (1990) pp. 157–169.
2. M. R. LAMBERT, R. G. HART and H. E. TOWNSEND, SAE paper, n°831817 (1983) pp. 1153–1159.
3. M. F. MATHIAS, C. M. VILLA and T. W. CHAPMAN, *J. of Applied Electrochem.* **20** (1990) 1.
4. A. SHIBUYA, T. KURIMOTO and M. KIMOTO, in "The Sumitomo search," **31** (1985) pp. 75–90.
5. L. FELLONI, R. FRATESI, E. QUADRINI and G. ROVENTI, *J. of Applied Electrochem.* **17** (1987) 574.
6. R. FRATESI and G. ROVENTI, *ibid.* **22** (1992) 657.
7. Y. L. CHEN and D. D. SNYDER, in "Zn-Based Steel Coating Systems: Metallurgy & Performance," edited by J. Krauss and D. K. Matlock (1990) pp. 95–107.
8. I. NENOV, I. GADSHOV and K. PANGAROV, *Galvanotechnik* **75** (1984) pp. 1107–1111.
9. A. SEKI and K. KAMEI, *ISIJ International* **32** (1992) 1306.
10. Y. OHMORI, K. KONDO, K. KAMEI and S. HINOTANI, Materials Research Society Symposia Proceedings **122** (1988) pp. 553–558.
11. K. KONDO, *Tetsu to Hagane* **77** (1991) 886.
12. T. B. MASSALSKI,"Metallic Solid Solutions," edited by J. Friedel and A. Guinier, (WA Benjamin Inc., NY, Amsterdam, 1963) p. XII.1–XII.15.
13. W. HEIKE, J. SCHRAMM and O. VAUPEL, *Metallwirtschaft* **XV** (1936) 655.
14. J. K. CRITCHLEY and S. DENTON, *J. of Inst. of Metals* **99** (1971) 26.
15. O. BARDIN, PhD thesis, Institut National Polytechnique, Toulouse-F (1995).

Received 17 December 1996
and accepted 27 August 1998